

Received 13 November 2019; accepted 12 January 2020. Date of publication 17 January 2020; date of current version 13 February 2020.  
The review of this article was arranged by Editor C. Bulucea.

Digital Object Identifier 10.1109/JEDS.2020.2967473

# Thermal Analysis of AlGa<sub>N</sub>/Ga<sub>N</sub> Hetero-Structural Gunn Diodes on Different Substrates Through Numerical Simulation

YING WANG<sup>1,2</sup>, LIU-AN LI<sup>3</sup>, CHONG LI<sup>4</sup>, JIN-PING AO<sup>2</sup>, XIAO WANG<sup>2</sup>, AND YUE HAO<sup>2</sup>

<sup>1</sup> School of Microelectronics, Northwestern Polytechnical University, Xi'an 710072, China

<sup>2</sup> State Key Discipline Laboratory of Wide Band Gap Semiconductor Technology, School of Microelectronics, Xidian University, Xi'an 710071, China

<sup>3</sup> School of Electronics and Information Technology, Sun Yat-sen University, Guangzhou 510275, China

<sup>4</sup> School of Engineering, University of Glasgow, Glasgow G12 8LT, U.K.

CORRESPONDING AUTHOR: J.-P. AO (e-mail: jpao@xidian.edu.cn)

This work was supported in part by the National Key Research and Development Program under Grant 2017 YFB043000, and in part by the National Science Foundation for Postdoctoral Scientists of China under Grant 2019M653554.

**ABSTRACT** GaN-based planar Gunn diodes are promising terahertz sources for monolithic microwave and terahertz integrated circuits (MMICs and MTICs, respectively) due to high output power and easiness of fabrication and circuit integration. However, high lateral current in the 2DEG channel may lead to failures such as early breakdown and suppression of oscillations. In this paper, we will, for the first time, systematically investigate the thermal effect on DC IV and output RF characteristics of AlGa<sub>N</sub>/Ga<sub>N</sub> hetero-structural planar Gunn diodes on different substrates including diamond, SiC, Si and sapphire. Our simulation results show that the best RF output performance comes with the devices on diamond substrate and no oscillating current is observed for devices on sapphire substrate. The suppress of Gunn oscillation in the device on sapphire is mainly due to the excessive heat generated in the channel that leads to increase of the dead zone and attenuation of electronic domains. These results will lay theoretical and experimental foundation for realizing not only milliwatt GaN-based terahertz semiconductor oscillators but also other power devices.

**INDEX TERMS** Wide band gap semiconductors, numerical simulation, terahertz Gunn diode, thermal effect.

## I. INTRODUCTION

Terahertz technology plays a significant role in the innovation of science and technology, and the development of national economy and national security. It has gained increasing attention and gradually occupied an important policy agenda [1]–[2]. Serious deficiencies of powerful terahertz radiation sources greatly restrict the development of terahertz and leads to terahertz as a “blank band” for a long term [3]. Recently, planar Gunn diodes as terahertz signal sources have been demonstrated and become a great potential for the sub-THz band applications, owing to its small size, low power consumption, high efficiency and low phase noise [4]–[5].

GaN-based Gunn diodes show even greater potential due to the high breakdown electric field and high electron drift velocity, especially in the applications of high-temperature

and high-power devices. Traditional Gunn devices are realized in vertical topology in which current flows through epitaxial layers which leads to high junction temperature and large package size [6]. On the contrary, planar Gunn devices in which current flows in parallel with epitaxial layers possess lower power density, better heat dissipation performance and higher working frequency [7]–[11].

In principle, the output RF power of a GaN planar Gunn diode could be up-to several hundred milliwatts in terahertz band [12]. The extremely high two-dimensional electron gas (2DEG) carrier concentration of GaN heterojunction also allows rapid formation of narrower electron domains in ultra-short channels of a few hundred nanometers that greatly increases oscillation frequency [13]. Furthermore, the simplified structure and easy integration of planar Gunn diode is compatible with the monolithic microwave and terahertz

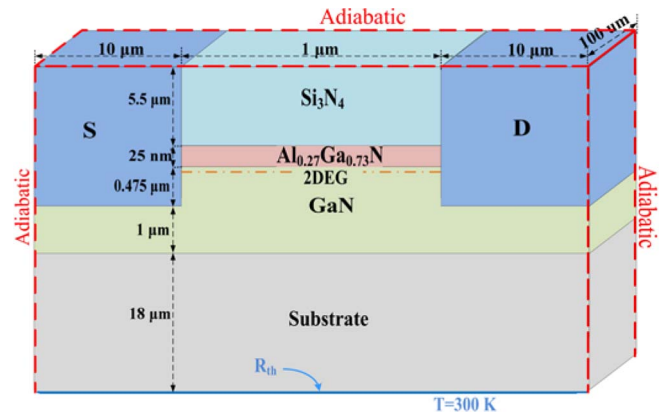
**TABLE 1.** Thermal parameters used in the simulation.

Material	$\kappa_{300}$ (W/cm·K)	$\alpha$	Heat capacitance $c$ (J/kg·K)	Mass density $\rho$ (kg/m <sup>3</sup> )
AlGa <sub>0.27</sub> N	0.25	-1.44	490	6070
GaN	1.6	1.4	490	6150
SiN	0.2	0	700	3000
Diamond	14.8	-0.55	520	3515
SiC	4.2	-1.3	581	3100
Si	1.5	-1.3	705	2329
Sapphire	0.35	-1	750 <sup>[23]</sup>	3960

integrated circuits (MMICs, MTICs). Therefore, GaN planar Gunn diodes are envisioned to be ideal terahertz radiation sources with high frequency and high power density in the band of 0.1 THz~2 THz [14].

Up to now, the quality of GaN material and device fabrication processes for power and optoelectronic devices have been significantly improved. However, there are still many challenges in realizing GaN Gunn diodes experimentally. At present, the reported Gunn effect observed in GaN experimentally are all achieved by using nanosecond pulsed voltage and high-speed oscilloscope to avoid heat generation [15], [16]. The self-heating phenomenon is one of the most important factors of restricting the realization of GaN-based Gunn diodes. The high temperature within GaN planar Gunn diodes will lead to attenuation of the electronic domains, which thus inhibits the negative resistance effect and greatly reduces RF output characteristics, or even suppress the oscillations [17]. Therefore, it is necessary to reduce the influence of heat generation in GaN Gunn diode for high frequency and high voltage operation. However, until now there is little research in this regard.

Some experimental techniques can be potentially used to evaluate the thermal characteristics of GaN hetero-structural devices, such as Raman spectroscopy, electrical measurement techniques, infrared IR thermal imaging, photoluminescence technique, thermo-reflectance thermography and infrared microscopy. However, those techniques are limited either by spatial or temperature resolution [18]. In addition, those techniques cannot measure the temperature distribution within the channel but the average temperature of the device. Numerical simulation is effective in this aspect because it provides a microscopic analysis on electron domain characteristics in the 2DEG channel and detailed distribution of the lattice temperature. In this work, we will study the thermal effect of the AlGa<sub>0.27</sub>Ga<sub>0.73</sub>N hetero-structural Gunn diode on different substrates by using a TCAD simulator. Our results show that the heat generated in the AlGa<sub>0.27</sub>Ga<sub>0.73</sub>N hetero-structural Gunn diode leads to increase of the dead zone and attenuation of electronic domains, which seriously deteriorate the output performance of the devices. Finally, we propose an optimized diamond substrate for minimizing the thermal effect and potentially realizing milliwatt GaN-based terahertz oscillators. In Section II, we introduce details of the simulation and the structure. In Section III, the results and discussion are reported. Conclusions are finally given in Section IV.

**FIGURE 1.** Schematic of the Al<sub>0.27</sub>Ga<sub>0.73</sub>N/GaN hetero-structural Gunn diode structure used in simulation.

## II. SIMULATION DETAILS

Two dimensional thermal simulations have been carried out by using the commercially available TCAD Silvaco Atlas. To simulate thermal effect, the standard heat flow equation is used and coupled to the primary drift-diffusion equations for simulating the Gunn effect. The heat flow equation has the following expression [19]:

$$\rho c \frac{\partial T}{\partial t} = \nabla \cdot \kappa \nabla T + j_n \cdot E$$

where  $c$  is the heat capacitance,  $\rho$  is the mass density,  $\kappa$  is the thermal conductivity,  $E$  is the electric field and  $j_n \cdot E$  is the joule heat generated by the electron current. Obviously, for a temperature time-invariant simulation,  $\nabla T / \nabla t$  becomes zero.

To improve accuracy, all materials used in the model have temperature-dependent thermal conductivities,  $\kappa(T)$ . The nonlinear thermal conductivity is modeled by employing Kirchhoff's transformation as:

$$\kappa(T) = \kappa_{300} / (T/300)^\alpha$$

where  $\kappa_{300}$  is the thermal conductivity at 300 K and  $\alpha$  is the temperature dependence coefficient. Other parameters for thermal simulation are provided in Table 1 [20]–[24].

Figure 1 illustrates the AlGa<sub>0.27</sub>Ga<sub>0.73</sub>N hetero-structural planar Gunn diode investigated in this study. The active region consists of a 1.475 μm GaN buffer and a 25 nm Al<sub>0.27</sub>Ga<sub>0.73</sub>N barrier layer. Both layers are assumed to be unintentionally doped and have a carrier concentration of  $1 \times 10^{15} \text{ cm}^{-3}$ .

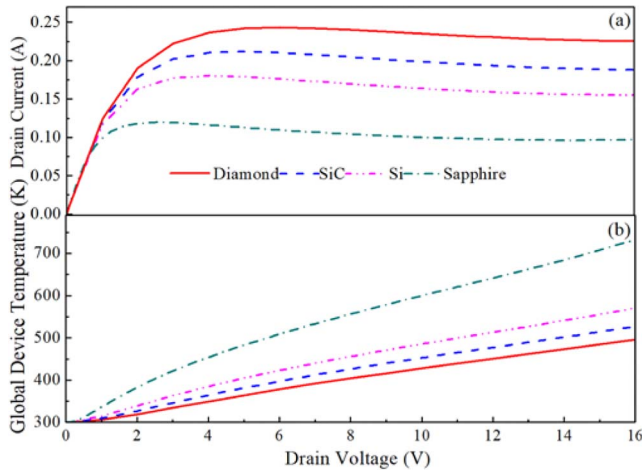


**FIGURE 2.** (a) Static I-V characteristics and (b) global device temperature vs. drain voltage for GaN Gunn diodes on different substrates with the same thickness of 18  $\mu\text{m}$ .

A 5.5  $\mu\text{m}$   $\text{Si}_3\text{N}_4$  layer is deposited on the top of the  $\text{Al}_{0.27}\text{Ga}_{0.73}\text{N}$  layer to improve the electrical performance of the device and protect the device surface during processing. Four types of substrates namely, diamond, SiC, Si, and sapphire are analyzed in this paper. The channel length between drain and source contacts,  $L_{\text{DC}}$ , is 1  $\mu\text{m}$ . If not otherwise specified, the length of drain and source contacts is always 1  $\mu\text{m}$  and the thickness of substrate is 18  $\mu\text{m}$ . Although thicker substrate helps to counterbalance the strain from upper epitaxial layers, it degrades heat dissipation (as shown in detail later) and leads to serious self-heating problem. In addition, thicker substrate greatly increases computing time. Therefore, we set the thickness to be 18  $\mu\text{m}$  which, in reality, can be realized by using either mechanical polishing or other chemical methods. The width of the device is 100  $\mu\text{m}$ . The thermal boundary settings are as follow: (i) All surfaces except the bottom surface of the device are set to be adiabatic. (ii) The heat transport from metal contacts to external surroundings is ignored to simplify the calculation and avoid the non-convergence problem. This is a common practice in the simulation of thermal effect as described in [25]–[27]. (iii) The ambient temperature is 300 K. (iv) To model both radiation energy loss and heat loss in the substrate, the thermal resistance  $R_{\text{th}}$  for different substrates is defined ( $R_{\text{th-diamond}} = 1.23 \times 10^{-8} \text{m}^2\text{K/W}$ ,  $R_{\text{th-SiC}} = 3.13 \times 10^{-8} \text{m}^2\text{K/W}$ ,  $R_{\text{th-Si}} = 4.69 \times 10^{-8} \text{m}^2\text{K/W}$ ,  $R_{\text{th-sapphire}} = 18.78 \times 10^{-8} \text{m}^2\text{K/W}$ ) [28]–[30].

### III. NUMERICAL RESULTS AND DISCUSSION

Firstly, we investigate the thermal effect on current characteristics and global device temperature for different substrates under DC bias conditions. The simulation results are shown in Fig. 2. It can be seen that the diamond substrate shows the best heat sinking capability because the device on-diamond shows the highest current and lowest global device temperature. On the contrary, the sapphire substrate reveals the worst heat sinking capability. When the bias voltage is 16 V,

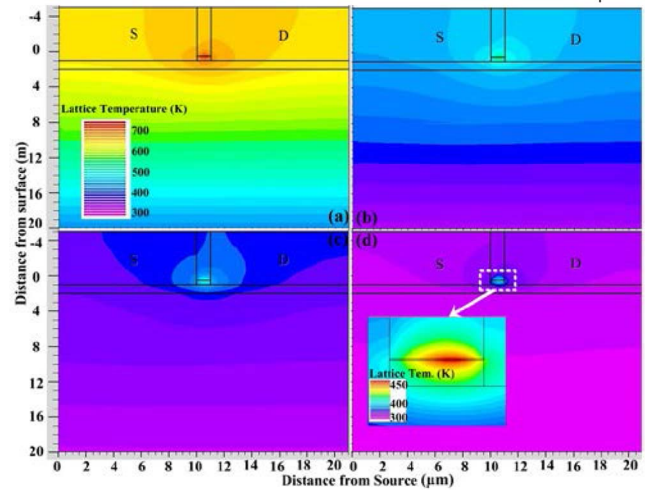


**FIGURE 3.** 2D distribution of the lattice temperature in Kelvin for the Gunn diode on (a) sapphire, (b) Si, (c) SiC, and (d) diamond (The bias between the drain and source is 16 V).

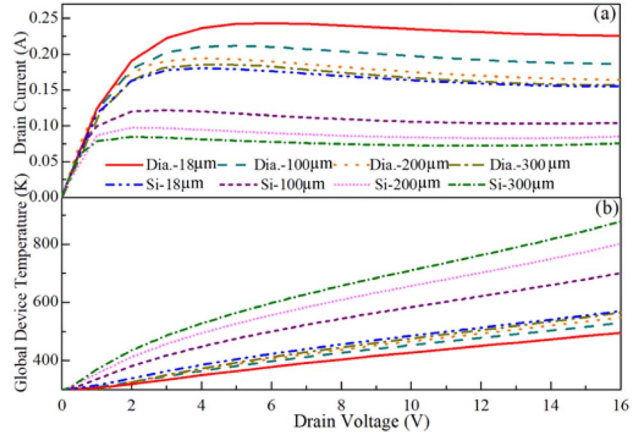


**FIGURE 4.** (a) Static I-V characteristics and (b) global device temperature vs. drain voltage for GaN Gunn diodes on Si and Diamond with different substrate thicknesses.

the global temperature of the device on-sapphire is about 732.26 K which is nearly 1.5 times higher than that of the device on-diamond. Fig. 3 represents the 2D lattice temperature distribution in the whole device on all four substrates and the inset in Fig. 3(d) shows temperature distribution of the channel region in the device on-diamond at 16 V. It is observed in Fig. 3 that the heat generated mainly concentrates in channel region. Because diamond has the highest thermal conductivity, the excessive heat generated in the channel can easily transfer to the bottom of the substrate and escape from the device; therefore, the overall temperature in the device decreases. The reduced channel temperature on the other hand reduces lattice scattering and thus the overall current is increased.

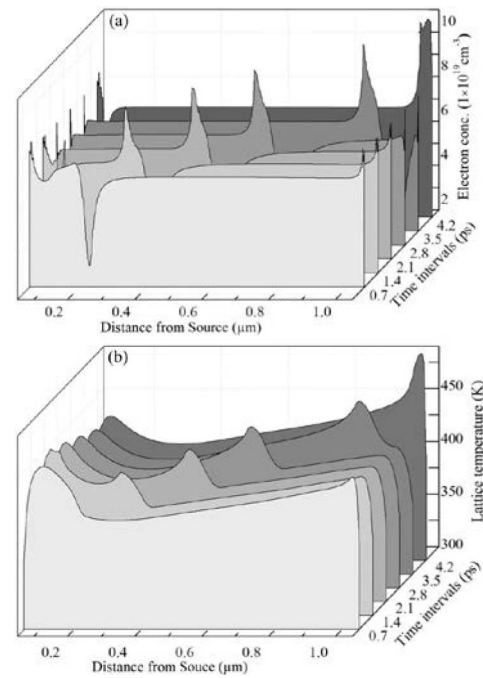
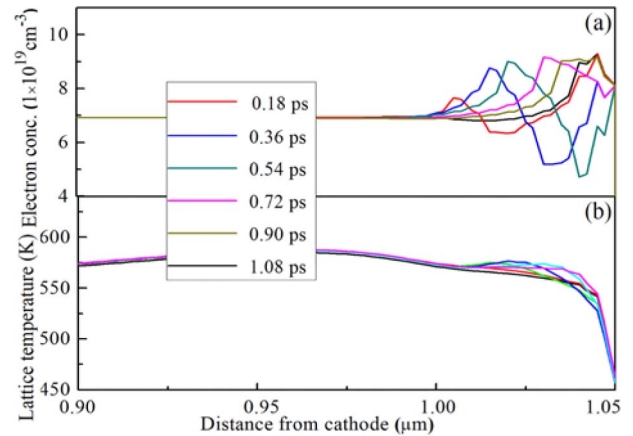
Secondly, we investigate how the thickness of substrate affects the global temperature and DC currents. The results are shown in Fig. 4. Four different thicknesses 18  $\mu\text{m}$ , 100  $\mu\text{m}$ , 200  $\mu\text{m}$ , and 300  $\mu\text{m}$  for both diamond and Si

**TABLE 2.** The RF output characteristics of the Gunn diodes on diamond, SiC and Si, respectively.

	Diamond	SiC	Si
$f$ (GHz)	236.8	420.1	895.1
$\eta$	1.167%	0.750%	0.035%
$P_{RF}$ (W)	0.037	0.027	0.002

substrates have been simulated. For device on Si, both the global temperature and the current change dramatically as increases of the thickness. All in all, 18  $\mu\text{m}$  shows the best performance. Thinner substrate is also possible however we must consider its mechanical strength for practical handling. For device on diamond the global temperature increases as the thickness increases and the current decreases quickly for the thickness increases from 18  $\mu\text{m}$  to 200  $\mu\text{m}$ . Further increase of thickness from 200  $\mu\text{m}$  to 300  $\mu\text{m}$  only decreases the current slightly. Fig. 3 confirms further the excellent heat dissipation capability of diamond. The effect of the thickness of diamond substrate on Gunn diode is relatively smaller than the thickness of Si substrates, which allows the Gunn diode to operate at thicker diamond substrates. Even if the thickness of the diamond substrate increases to 300  $\mu\text{m}$ , the device still generates higher current and lower operation temperature than the device on 18- $\mu\text{m}$  Si.

Thirdly, we studied oscillation characteristics of the Gunn diode on different substrates and the simulation results are shown in Fig. 5. Stable oscillations are observed in the device on diamond, SiC and Si. However, no oscillating current is seen in the device on-sapphire. This is mainly due to the excessive heat accumulated in the channel. We have also noticed that for devices on Si when the thickness of the substrate is greater than 100  $\mu\text{m}$  Gunn domains are on longer able to form in the channel. However, the Gunn diode on 300- $\mu\text{m}$  diamond shows better RF characteristics than the diode on 18- $\mu\text{m}$  Si. Other RF results including oscillation frequency  $f$ , RF-to-DC conversion efficiency  $\eta$  and RF power  $P_{RF}$  for devices on diamond, SiC and Si are shown in Table 2. It is evident that due to the poorer heat sinking capability of SiC, and Si substrate,  $\eta$  and  $P_{RF}$  drops greatly as compared with the device on diamond. This is because the electron velocity decreases as temperature increases, which results in the decrease of current as shown in Fig. 2 (a). However, the frequency of the device on SiC and Si increases. To prove this, we have extracted electron concentration and lattice temperature profiles at the same time intervals during one oscillation circle from the Gunn diode on diamond (Fig. 5) and from the diode on Si (Fig. 6). As illustrated in Fig. 5, the dipole domain forms inside the 2DEG channel of the Gunn diode on diamond, and each lattice temperature peak corresponds to a domain. Temperature increases as the dipole domain grows; therefore, as the domain reaches the drain contact, the lattice temperature increases to its highest point. However, for the Gunn diode on Si, there are only small dipole domain formed near the drain contact and the lattice temperature peaks mainly

**FIGURE 5.** (a) The electron concentration and (b) lattice temperature distribution profiles of the Gunn diode on diamond derived at the same time intervals inside one oscillation circle.**FIGURE 6.** (a) The electron concentration and (b) lattice temperature distribution profiles of the Gunn diode on Si derived at the same time intervals inside one oscillation circle.

near the drain contact as illustrated in Fig. 6. The dead zone is greatly elongated due to the thermal effect. Thus, the actual travel distance of the domain is in fact shorten therefore the oscillation frequency is increased up to 895.1 GHz. However, the downside of the extension of the dead zone is the increase of the channel resistance which also results in the decrease of  $\eta$  and  $P_{RF}$ . Based on the results above, we can conclude that it is an effective method to solve the thermal effect in the GaN device by fabricating the device on the diamond substrate. To realize the GaN HEMT on diamond, the most commonly used process is the technique of diamond substrate transfer [31]–[32].



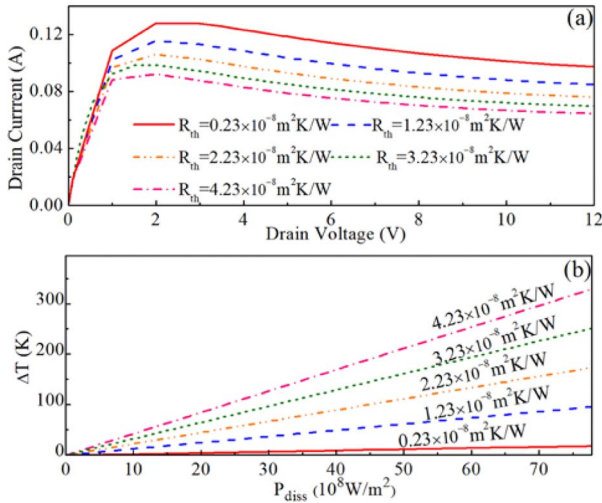


**FIGURE 7. (a) Static I-V characteristics and (b) substrate temperature rise ( $\Delta T$ ) vs. DC power dissipated within the channel for the Gunn diode on diamond (where  $I_D = I_S = 0 \text{ } \mu\text{m}$ ).**

We also study the effect of thermal resistance on the Gunn effect for devices on diamond substrate. The thermal resistance is an important parameter to estimate the lattice temperature of the device. In AlGaIn/GaN hetero-structural Gunn diode, the generated heat mainly transfers from the channel towards to the bottom of the substrate. The heat transfer capability of the substrate can be calculated by the equivalent thermal resistance  $R_{th}$ . Lower  $R_{th}$  can improve the device performance.  $R_{th}$  mainly depends on the thermal conductivity of the substrate. The higher the thermal conductivity is, the lower the  $R_{th}$  is. The device grown on diamond substrate has lowest thermal resistance ( $R_{th\text{-diamond}} = 1.23 \times 10^{-8} \text{ m}^2\text{K/W}$ ). The thermal resistance is affected by the lattice quality and varies significantly reported in the literature depending on measurement methods implemented. We therefore investigate how different  $R_{th}$  may affect the performance of the Gunn diode.  $R_{th}$  is swept from  $1.23 \times 10^{-8} \text{ m}^2\text{K/W}$  to  $4.23 \times 10^{-8} \text{ m}^2\text{K/W}$  with steps of  $1 \times 10^{-8} \text{ m}^2\text{K/W}$ . The length of drain and source contacts are set to be zero. As seen in Fig. 7(a), when  $R_{th}$  increases, the current decreases. In theory, the temperature change of bottom surface of the substrate  $\Delta T$  is defined as:  $\Delta T = T - T_0 = P_{diss} \cdot R_{th}$ , where:  $P_{diss} = V_{DC} \cdot I_{DC}$  is the DC power dissipated within the channel,  $T$  is the lattice temperature of the bottom surface of the substrate,  $T_0$  denotes a reference temperature of 300 K. Based on the static I-V characteristics showed in Fig. 7(a), we can work out the DC power dissipated  $P_{diss}$ . Fig. 7(b) shows the temperature change  $\Delta T$  as a function of DC power dissipated  $P_{diss}$ . The thermal resistance  $R_{th}$  can be extracted from the slope of the curves in Fig. 7(b) as  $R_{th} = d\Delta T/dP_{diss}$ . It can be seen that the thermal resistance  $R_{th}$  extracted by this method is in good agreement with theoretical values.

Finally, we compare the I-V characteristics and the thermal effect under DC and pulsed conditions for Gunn diode on diamond. Drain voltage pulse widths are  $1 \times 10^{-10} \text{ s}$ ,

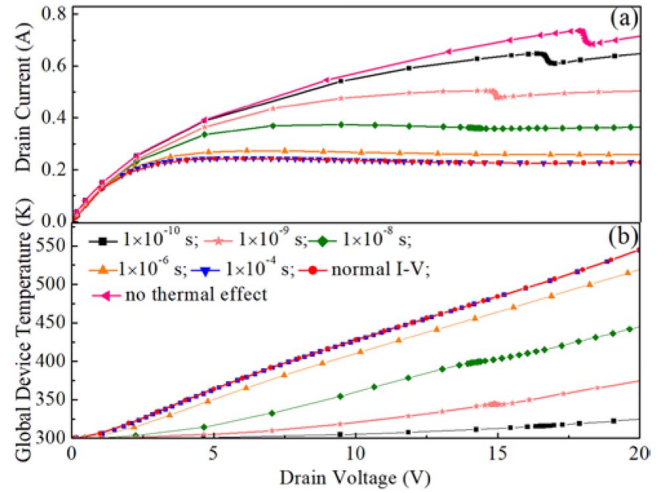


**FIGURE 8. (a) Pulsed I-V characteristics at different pulse widths and (b) the corresponding global device temperature vs. drain voltage for the Gunn diode on diamond.**

$1 \times 10^{-9} \text{ s}$ ,  $1 \times 10^{-8} \text{ s}$ ,  $1 \times 10^{-6} \text{ s}$  and  $1 \times 10^{-4} \text{ s}$ . The I-V curve without considering thermal effects is given in Fig. 8 (a). As illustrated in the graph, drain currents show slight variations at smaller drain voltage, this is because the power generated is not high enough to heat up the channel; therefore the thermal effect can be ignored in this case. However, at higher drain voltage, drain current decreases as pulse width increases, but it tends to become stable. Without taking the thermal effect into consideration or as the pulse width  $t \leq 1 \times 10^{-8} \text{ s}$ , the I-V curves show obvious negative differential resistance effect, which weakens as  $t$  increases. When pulse width  $t = 1 \times 10^{-4} \text{ s}$ , the I-V curve almost coincides with the I-V curve under DC condition, so does the global device temperature profiles as shown in Fig. 8(b). Yilmazoglu *et al.* [16] observed a stable NDR region on the pulsed I-V curve at 40 ns pulse width for vertical GaN Gunn diode devices on GaN substrate, which further demonstrates that effective suppression of heat generation is a key for obtaining stable Gunn oscillation.

#### IV. CONCLUSION

The thermal effect on the performances of AlGaIn/GaN hetero-structural Gunn diode on different substrates has been investigated using a numerical method. It can be concluded that the heat generation in the channel could be the key limiting factor for GaN-based Gunn diode. In order to realize stable GaN-based Gunn diode, it is necessary to effectively suppress heat generation in the channel or improve heat dissipation performance of the device. Diamond substrate with the highest thermal conductivity among all four substrates and therefore, the best DC and RF performance are achieved with the Gunn diode on diamond. The oscillation frequency  $f$  of  $1 \text{ } \mu\text{m}$  Gunn diode on diamond is as high as 236.8 GHz, with a RF-to-DC conversion efficiency of 1.167% and RF power of 37 mW. However, no oscillating current is observed in the Gunn diode on sapphire because the global device

temperature exceeds 700 K. We also found that reducing thermal resistance is an effective method to suppress self-heating effect. The thermal resistances extracted from the Gunn diode on diamond are in good agreement with the theoretical values. Furthermore, we also prove that the narrow pulse width, e.g., nanoseconds help to reduce heat accumulation in the channel; therefore, to realize the GaN Gunn diode experimentally.

## REFERENCES

- [1] T. Nagatsuma, "THz communication systems," in *Proc. IEEE Opt. Fiber Commun. Conf. Exhibit*, Los Angeles, CA, USA, Mar. 2017, Paper Tu3B.1.
- [2] F. Topfer and J. Oberhammer, "Millimeter-wave tissue diagnosis: The most promising fields for medical applications," *IEEE Microw. Mag.*, vol. 16, no. 4, pp. 97–113, May 2015, doi: [10.1109/MMM.2015.2394020](https://doi.org/10.1109/MMM.2015.2394020).
- [3] H.-J. Song and T. Nagatsuma, *Handbook of Terahertz Technologies (Devices and Applications)*. Boca Raton, FL, USA: CRC Press, 2015.
- [4] M. S. Shur and V. Ryzhii, "Emerging solid state terahertz electronics," *Terahertz Sources and Systems*, R. E. Miles, P. Harrison, and D. Lippens, Eds. Dordrecht, The Netherlands: Kluwer, 2001.
- [5] F. Amir, C. Mitchell, N. Farrington, and M. Missous, "Advanced Gunn diode as high power terahertz source for a millimetre wave high power multiplier," in *Proc. Int. Soc. Opt. Eng. (SPIE)*, vol. 7485, 2009, pp. 748–501.
- [6] C. Zhong, J. Xu, Z. Yu, and Y. Zhu, "Ka-band substrate integrated waveguide Gunn oscillator," *IEEE Microw. Wireless Compon. Lett.*, vol. 18, no. 7, pp. 461–463, Jul. 2008.
- [7] A. Khalid *et al.*, "A planar Gunn diode operating above 100 GHz," *IEEE Electron Device Lett.*, vol. 28, no. 10, pp. 849–851, Oct. 2007.
- [8] C. Li *et al.*, "Enhancement of power and frequency in HEMT-like planar Gunn diodes by introducing extra delta-doping layers," *Microw. Opt. Compon. Lett.*, vol. 53, no. 7, pp. 1624–1626, 2011.
- [9] A. M. Song, M. Missous, P. Omling, A. R. Peaker, L. Samuelson, and W. Seifert, "Unidirectional electron flow in a nanometer-scale semiconductor channel: A self-switching device," *Appl. Phys. Lett.*, vol. 83, no. 9, pp. 1881–1883, 2003.
- [10] N. J. Pilgrim, A. Khalid, G. M. Dunn, and D. R. S. Cumming, "Gunn oscillations in planar heterostructure diodes," *Semicond. Sci. Technol.*, vol. 23, no. 7, 2008, Art. no. 075013.
- [11] S. Pérez, J. Mateos, and T. González, "Submillimeter-wave oscillations in recessed InGaAs/InAlAs heterostructures: Origin and tunability," *Acta Physica Polonica*, vol. 119, no. 2, pp. 111–113, 2011.
- [12] V. N. Sokolov, K. W. Kim, V. A. Kochelap, and D. L. Woolard, "Terahertz generation in submicron GaN diodes within the limited space-charge accumulation regime," *J. Appl. Phys.*, vol. 98, no. 6, pp. 1–7, 2005.
- [13] B. Aslan and L. F. Eastman, "A THz-range planar NDR device utilizing ballistic electron acceleration in GaN," *Solid-State Electron.*, vol. 64, no. 1, pp. 57–62, 2011.
- [14] Y. Wang *et al.*, "Ultra-short channel GaN high electron mobility transistor-like Gunn diode with composite contact," *J. Appl. Phys.*, vol. 116, no. 9, 2014, Art. no. 094502.
- [15] Z. C. Huang, R. Goldberg, J. C. Chen, Y. Zheng, D. B. Mott, and P. Shu, "Direct observation of transferred-electron effect in GaN," *Appl. Phys. Lett.*, vol. 67, no. 19, pp. 2825–2826, 1995.
- [16] O. Yilmazoglu, K. Mutamba, D. Pavlidis, and T. Karaduman, "Measured negative differential resistivity for GaN Gunn diodes on GaN substrate," *Electron. Lett.*, vol. 43, no. 8, pp. 480–482, 2007.
- [17] Y. Wang, J. P. Ao, S. B. Liu, and Y. Hao, "Thermal modeling of the GaN-based Gunn diode at terahertz frequencies," *Appl. Sci.*, vol. 9, no. 1, p. 75, 2019.
- [18] A. Darwish, A. J. Bayba, and H. A. Hung, "Channel temperature analysis of GaN HEMTs with nonlinear thermal conductivity," *IEEE Trans. Electron Devices*, vol. 62, no. 3, pp. 840–846, Mar. 2015.
- [19] *Atlas User's Manual*; Silvaco International Software, Atlas, Santa Clara, CA, USA, 2014.
- [20] J. Das *et al.*, "Improved thermal performance of AlGaIn/GaN HEMTs by an optimized flip-chip design," *IEEE Trans. Electron Devices*, vol. 53, no. 11, pp. 2696–2702, Nov. 2006.
- [21] J. E. Butler and A. V. Sumant, "The CVD of nanodiamond materials," *Chem. Vapor Deposition*, vol. 14, nos. 7–8, pp. 145–160, 2008.
- [22] H. I. Fujishiro, N. Mikami, and M. Hatakenaka, "Monte Carlo study of self-heating effect in GaN/AlGaIn HEMTs on sapphire, SiC and Si substrates," *Physica Status Solidi C*, vol. 2, no. 7, pp. 2696–2699, 2005.
- [23] H. Guo, Y. Kong, and T. Chen, "Thermal simulation of high power GaN-on-diamond substrates for HEMT applications," *Diamond Related Mater.*, vol. 73, pp. 260–266, Mar. 2017.
- [24] D.-M. Liu, W. H. Tuan, and C.-C. Chiu, "Thermal diffusivity, heat capacity and thermal conductivity in Al<sub>2</sub>O<sub>3</sub>-Ni composite," *Mater. Sci. Eng. B*, vol. 31, no. 3, pp. 287–291, May 1995.
- [25] A. K. Sahoo *et al.*, "Thermal analysis of AlN/GaN/AlGaIn HEMTs grown on Si and SiC substrate through TCAD simulations and measurements," in *Proc. Microw. Integr. Circuits Conf.*, London, U.K., Oct. 2016, pp. 145–148.
- [26] S. García, I. Íñiguez-de-la-Torre, J. Mateos, T. González, and S. Pérez, "Impact of substrate and thermal boundary resistance on the performance of AlGaIn/GaN HEMTs analyzed by means of electro-thermal Monte Carlo simulations," *Semicond. Sci. Technol.*, vol. 31, no. 6, 2016, Art. no. 0650056.
- [27] J. P. Jones, E. Heller, D. Dorsey, and S. Graham, "Transient stress characterization of AlGaIn/GaN HEMTs due to electrical and thermal effects," *Microelectron. Rel.*, vol. 55, no. 12, pp. 2634–2639, Dec. 2015.
- [28] S. García, I. Íñiguez-de-la-Torre, Ó. García-Pérez, J. Mateos, T. González, and S. Pérez, "Modelling of thermal boundary resistance in a GaN diode by means of electro-thermal Monte Carlo simulations," *J. Phys. Conf. Ser.*, Euro-TMCS I: Theory, Modelling and Computational Methods for Semiconductors, vol. 609, May 2015, Art. no. 012005.
- [29] J. Wu, J. Min, W. Lu, and P. K. L. Yu, "Thermal resistance extraction of AlGaIn/GaN depletion-mode HEMTs on diamond," *J. Electron. Mater.*, vol. 44, no. 5, pp. 1275–1280, 2015.
- [30] R. Rodríguez *et al.*, "Numerical simulation and compact modelling of AlGaIn/GaN HEMTs with mitigation of self-heating effects by substrate materials," *Physica Status Solidi A Appl. Mater.*, vol. 212, no. 5, pp. 1130–1136, 2015, doi: [10.1002/pssa.201431897](https://doi.org/10.1002/pssa.201431897).
- [31] P.-C. Chao *et al.*, "Low-temperature bonded GaN-on-diamond HEMTs with 11 W/mm output power at 10 GHz," *IEEE Trans. Electron Devices*, vol. 62, no. 11, pp. 3658–3664, Nov. 2015.
- [32] K. Chu, P. C. Chao, and T. Carlton, "Creamer method for gallium nitride on diamond semiconductor wafer production," U.S. Patent 14 800 387, 2015.